MAGNETOELASIC SENSORS FOR THE REAL-TIME TRACKING OF MSC GROWTH

by

SUNNY ZHANG

A THESIS

Presented to the Department of Biology
and the Robert D. Clark Honors College
in partial fulfillment of the requirements for the degree of
Bachelor of Science

February 2022

An Abstract of the Thesis of

Sunny Zhang for the degree of Bachelor of Science
in the Department of Biology to be taken March 2022

Title: Magnetoelastic Sensors for the Real-Time Tracking of MSC Growth

Approved: *Keat Ghee Ong, Professor of Knight Campus*
Primary Thesis Advisor

The cell therapeutics industry has grown significantly in the past decade; however, in adherent cell cultures, there is still a technological gap for a non-invasive, scalable, method of tracking cell-number and critical process parameters remotely and in real-time. Magnetoelastic sensors can be manipulated remotely with magnetic fields to monitor different physical, chemical, and biological parameters. Fabrication of these sensors can also be scaled into different sizes to be used in chemical and biological sensing, making them a promising prospect in tracking the growth of human-derived Mesenchymal stromal/stem cells (hMSCs) in real-time. In this study, we develop a sensing platform that uses magnetoelastic materials to monitor MSC growth/numbers in 2D *in vitro* cell cultures. Cultured MSCs are seeded onto a magnetoelastic sensor, which is then excited by an alternating magnetic field that causes the sensor to resonate and generate a magnetic flux. The basis for this research is supported by previous studies with magnetoelastic sensors that have shown the capability of measuring the cell numbers of L929 fibroblasts. This study intends to continue the development of the sensing platform for the purpose of remotely tracking MSC growth in real-time. The technology being developed will offer a more robust and scalable approach for monitoring and manufacturing stromal/stem cells in a consistent manner.

Acknowledgements

I would like to thank Dr. Keat Ghee Ong and William Skinner for mentoring and supporting me along the examination of this study. Through their expertise and knowledge, I was able to consider various perspectives and contexts related to this subject matter, assisting in the investigation and content of this paper. I would also like to thank Salil Karipott for training me on various skills and procedures needed during the development of this paper. I would also like to extend my thanks to Jasmine Garcia and the Guldberg lab for assisting in cell culturing and providing the cell media for this paper. Finally, I would like to thank Dr. Keat Ghee Ong, Dr. Corinne Bayerl, and Dr. Annie Zemper for taking the time and dedication to serve as members of my thesis committee.

Table of Contents

List of Figures

Introduction:

Mesenchymal Stromal/Stem Cells (MSCs) and its Current State in Regenerative Medicine

Differentiated cells are the final forms of cells that have their own specialized function. Examples include muscle cells which function to turn certain chemicals into mechanical energy so that our muscle fibers can contract, nerve cells that receive and send signals from and to the central nervous system, and bone cells that are responsible for forming bone and the supporting structure to support locomotion. These specialized cells vary in their functions and location but remain vital in maintaining stability within our bodies. However, the production of these specialized cells depends on stem cells. Stem cells act as building blocks to specialized cells. They are capable of self-renewal and differentiate (or specialize) based on cellular signals and parameters present during their production and growth. These cells can either be pluripotent or multipotent, meaning they can give rise to a whole new organism or into most cell types of an organism. This feature makes them essential in an organism's natural development and healing process. Particularly in healing, stem cells can replace or provide specialized cells that have been damaged and/or are missing. However, stem cells either become restricted in their specialization potential or become limited in quantity as the organism gets older. This limitation can hinder how effectively the body can respond to certain injuries or diseases that attack and damage cells in older adults. In response to this, the field of regenerative medicine was developed to use human extracted stem cells - known as human-derived stem cells - to repair damaged cells and tissues that other

forms of treatment can't repair. By harvesting, growing, and producing viable cells for transplantation, this method known as stem cell therapy, aims to repair and treat prevalent injuries and diseases by taking advantage of cells' inherent ability to self-renew and differentiate into specialized cells [3].

The past decade has seen immense funding and research in stem cells to expand their use in treatments and therapeutics due to their vast potential in regenerative medicine [14]. Of those examined, mesenchymal stromal/stem cells (MSCs) have become some of the most promising candidates due to their immunosuppressive capabilities and capacity to differentiate into mesodermal -i.e. bone, cartilage, and fat - , ectodermal - i.e. skin, hair, and nails - , and endodermal cell types – i.e. heart muscle, liver, nerve, and skin [9]. MSCs express stem-like characteristics such as self-renewal and multilineage differentiation [9]; however, because there have been studies indicating that MSCs aren't fully "stem cells", they are sometimes referred to as "stromal cells" instead of "stem cells". For consistency and to avoid wrongful terminology, they will be referred to as either MSCs or "adherent cells".

MSCs are widely available from multiple sources in the body – such as bone marrow, adipose tissue, limb bud, and dental tissues. Using low-risk techniques, MSCs can be extracted and cultured for transplantation in cell therapy to treat different disorders/diseases that affect millions of people – such as bone and cartilage disorders, heart disease, and neurological disorders [9]. Current research and clinical studies using human-derived MSCs (hMSCs) have already investigated the promise that these cells hold in treating a wide range of ailments; however, limitations exist in the effectiveness and reliability of producing the final products of MSCs [22] whether it be for research

purposes or cell therapy. Current methods in tracking the growth, concentration, and conditions of MSC cultures during their production are time-consuming and labor-intensive. These processes could also destroy the therapeutic potential of these desired MSC products [12]. These limitations could slow the development and research of MSCs and their use as a therapeutic.

Current MSC Culturing and Tracking Techniques

After extraction and isolation, MSCs are typically cultured onto conventional monolayer (2D) cultures – such as on a petri dish – to expand/grow the limited number of isolated adherent cells. However, growing evidence emphasizes the limitations of expanding adherent cells on monolayer cultures due to the limited control and increased risk of contamination [18]. Recent advancements in adherent cell expansion look towards growing MSCs in suspension (3D) cultures - such as microcarrier-based bioreactors - to generate a high production of MSCs while also being able to control the culture parameters to effectively produce quality products [18]. However, a vital component in this process is monitoring and tracking the cell growth to ensure that culture parameters are optimized for the creation of a quality product. Current cell-tracking methods, while optimal, are either non-applicable to bioreactor cultures or can be limited in their productivity, cost, and ability to monitor cells in real-time. For instance, microscopy-based-tracking techniques that could offer cell tracking in real-time with minimal invasion in 2D cultures, don't apply to bioreactor cultures due to the three-dimensional structure and optical properties of the microcarriers that MSCs are grown on [19].

Other methods of tracking cell growth that are currently used rely on more invasive techniques, and although they are effective, are limited by their potential to introduce error and contamination. Monitoring techniques that involve detaching MSCs from their carriers or injecting fluorescent dyes are a common and effective method used to monitor cell growth; however, these techniques tend to render the cells unsuitable for therapeutic applications – generating unneeded waste [11]. Additionally, some visual image processing systems, such as optical imaging and radionuclide imaging, also tend to lack the ability to monitor every desired aspect of the adherent cell culture [20] while also putting cultures at risk of other factors such as radiation [2]. With hMSCs having to originate from human donors, these forms of monitoring techniques can lead to the waste of an already limited resource and the slow production of a desired therapeutic.

Additionally, these current forms of cell monitoring lack the capability to track these cell cultures in real-time. The ability to track cells in real-time is a key benefit in this approach because it provides a route to automated feedback-control processes - which can be employed to stabilize and control parameters and conditions that could affect the cells produced. Without this technology, cell manufacturers would rely on manual techniques that could be unreliable and insufficient for producing MSCs at high volumes. Considering how quickly cell therapy is developing and needed for treating debilitating disease, there is a need for a more robust and reliable method of monitoring hMSCs and critical process parameters (CPPs) in real-time to facilitate the production of larger quantities of adherent cells that are consistently reproducible while also ensuring safety and quality in the final product [12].

Magnetoelastic Sensors: Potential for Real-Time Monitoring of Biological and Chemical Parameters

Magnetoelastic (ME) sensors are a potential alternative in remotely monitoring MSC cultures in real-time with minimal invasion while also being controllable, reducing the probability of procedural and tracking errors. ME sensors are fabricated from magnetoelastic materials, typically composed of amorphous ferromagnetic ribbons, which are inexpensive metals –providing a low-cost, scalable, and available resource [17]. ME materials are inherently high in magnetostriction and magnetoelastic coupling[17]. These are properties that describe a magnetic material's property of change after magnetization and energy conversion [17]. High magnetoelastic couple and magnetostriction allow the conversion of magnetic energy to mechanical energy and vice versa -, causing physical deformations and generating a mechanical resonance when exposed to a magnetic field [8]. An external magnetic field applied to ME material causes it to produce longitudinal vibrations that convert to elastic waves and generate a magnetic flux at a characteristic resonance frequency. This magnetic flux can be detected remotely as a resonance frequency through detection systems.

The property of ME material to generate a returning signal at a characteristic resonance frequency makes them an optimal medium for a sensor that can measure a range of biological and chemical parameters. Any mass change or loading onto the sensors can change the resonance frequency produced by the sensor (fig. 1). Even environmental changes of the cell cultures, such as temperature changes, can affect the vibration of the sensor and be detected. Resonance of the sensor can be affected by the system that it is placed in, and any changes in resonance can be accredited to changes in

the system. This can be compared to a very sensitive scale – such as a quartz crystal microbalance – in which any change in the mass or parameters results in the scale indicating a change or difference on the scale. This responsive behavior allows the material to not only detect and measure physical parameters - such as pressure, temperature, and liquid density - but can also be functionalized for chemical and biological sensing [6]. Thus, ME sensors could be used to provide real-time measurements of cell numbers and CPPs non-invasively via externally applied and detected magnetic fields. However, to date, ME sensors have mainly been tested with bacterium and other prokaryotic cultures – which are unicellular. hMSCs, though, are eukaryotic, and only recently have these ME sensors been studied to have the capability to monitor the growth of mammalian cells - L929 Fibroblasts - in real-time [21]. The intention of this study, then, is to both expand upon current cell tracking methods and extend current works on the functionality of magnetoelastic sensors for hMSC tracking. The goal of this study is to develop and show proof of concept for a ME sensor-based cell tracking system that generates consistent, reliable, information about MSC growth conditions and cell parameters for the intended use of producing optimal final products – in terms of quantity and quality. Proof of concept for such a system is necessary for validating its functionality and plausibility and will be done so through the fabrication of the ME sensors, the seeding of MSC onto the sensors, the calibration of the measurement system, and the data collected.

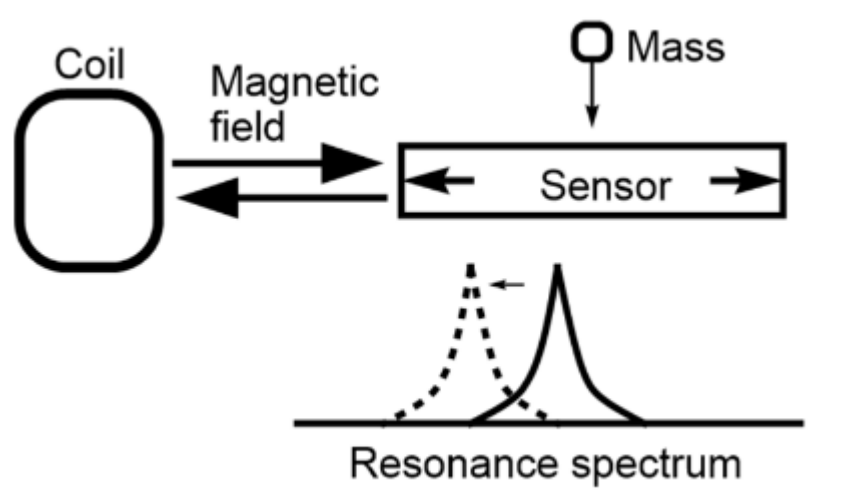

Figure 1: Mass loading onto ME sensors create a shift in the resonance frequency of the ME sensor

ME sensors generate a characteristic resonance frequency when an external magnetic field is applied to it. The loading or mass change of the ME sensor can create a shift in its characteristic resonance due to a dampening effect by the loading.

Broader Implications of this Research

Currently, MSCs have been studied in regenerative medicine to be used in bone regeneration, cartilage repair, central nervous system repair, cardiac disease, and liver regeneration [7]. Injuries such as bone fractures affect 178 million new individuals as of 2019 and diseases such as cardiac disease affected 16.3 million Americans in 2011 [10] while also being the leading cause of death in the United States [1]. These prevalent diseases affect the lives of many, being an obstruction or a hindrance to daily activities. Additionally, these prevalent injuries and diseases are costly, not only to the individuals but also to the economy. As of 2022, treatment for knee cartilage defects and fractures ranged from $50,000 to $120,000 [4]. Outside of individual costs, healthcare costs for the treatment and loss of productivity in the long-term halt the progress and growth of the economy [10]. While stem cell treatments do currently exist, current models value these treatments ranging from $10,000 to $50,000 [23], a cost that could be exponentially lowered if improvements in the yield and quality of its products were made [17]. This study aims to advance techniques for MSC research and manufacturing by eliminating wastefulness and procedural errors that may occur. Although current methods of cell monitoring are the gold standards in cell tracking and characterization, they can be limited in their efficiency and applicability to different culture settings. The intention of this study is to create an alternative tool in this field and the development of further tracking systems using ME sensors. This could lead to faster developments in the field of stem cell research that could ultimately benefit the field of regenerative medicine.

Materials and Methods:

ME Sensor Fabrication

Fourteen magnetoelastic (ME) sensors were needed for this study. Eight ME sensors were designated to be used for studying the resonance and impedance of the sensors in relation to MSC growth, the other six sensors were used to study the effects gelatin soaking had on MSC attachment onto the ME sensor surface. The ME sensors were fabricated to be 12.7 mm x 5 mm from commercially available magnetoelastic material (Metglas 2826MB) by mechanically shearing them lengthwise with a commercial paper cutter. Once sheared, the ME sensors were annealed at 125ºC for 2 hours in a gravity convection lab oven (Quincy Lab 10GC) to buffer out rough edges and generate a uniform surface for cell attachment. Annealed sensors were then coated with 10 μm of thick Parylene-C conformal layer (PDS 2010 Labcoater, SCS) using a SCS Labcoter 2 Parylene Deposition System to allow the sensor to be biocompatible in *in vivo* environments. Coated sensors were finally treated with oxygen plasma in a reactive etching system (March Jupiter II RIE system) for 30 s at 100 W to increase cell adhesion on the surface of the sensor, generating a completed ME sensor.

Sensor Detection System

The sensor detection system consisted of a two-coil system: a DC coil and an AC coil. The DC coil was designed using a 3D CAD software (Autodesk Fusion360) to be a 30 mm x 50 mm cylindrical coil. The design was then 3D printed using a 3D printer (Lulzbot Taz). Once printed, the coil was wound with an 18-gauge AWG magnet wire using a mechanical (Adams-Maxwell 1201-3AR Bench-top coil winder)

for 50 turns. Once completely wound and assembled, the DC coil was placed into a 3D printed coil holder and connected to a power supply/DC generator (Kepco Programmable Power Supply) to generate a DC magnetic field. The AC coil was then assembled, using the same 3D CAD software and 3D printer to design and print the coil. The AC coil was designed to be 30 mm x 50 mm and was wound with 32-gauge AWG magnet wire for 180 turns. Once wound, a connection was soldered onto the coil that allowed the connection of the AC coil and the impedance analyzer (Keysight E5061B Network Analyzer) that it was connected to. The AC was used to produce an AC magnetic field that excites and measures the frequency response of the sensor. This response was analyzed and controlled through the impedance analyzer. The completed system can be seen in Figure 2.

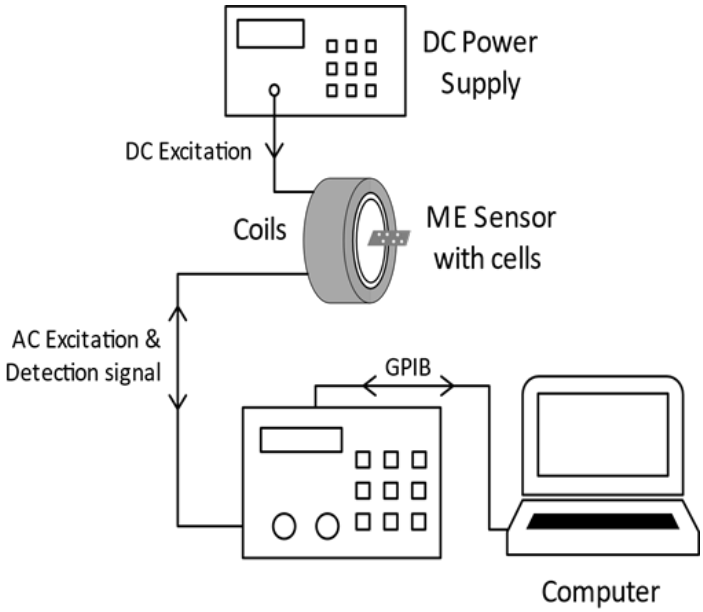

Figure 2: Schematics of the measurement system used to monitor the ME sensors

The ME sensor detection system will consist of a DC and AC coil. The DC coil was connected to a DC power supply to generate a DC magnetic field. The AC coil was be connected to a Impedance analyzer and computer to detect and measure the frequency response of the sensor.

Carrier Stage Construction

Using a 3D CAD software (Autodesk Fusion 360), fourteen carrier stages were designed for the intention of holding the ME sensors - that would be seeded with MSCs - in place and in partial suspension within the chamber slide. The carrier stage was designed to be 22.0 mm x 18.0 mm x 2.0 mm with a 14.00 mm x 7.00 mm x 0.87 mm indentation in the center intended to hold the ME sensor. The carrier stage design was processed using 3D printing software (PreForm) and 3D printed using a FormsLab Form 2 3D printer from High Temp V2 resin. After printing, the carrier stages were

washed and cured in a Form Wash and Form Cure for post-print processing. After post-print processing, supports printed onto the carrier stages were removed by mechanical cutting.

Sensor and Carrier Stage Sterilization

To ensure that no byproducts or containments that could affect MSC growth were present on the ME sensors or carrier stages during the cell seeding process, all of the ME sensors and carrier stages fabricated were placed within an autoclaved through a steam cycle for 30 minutes.

MSC Culturing

hMSCs were used for all *in vitro* cell cultures. hMSCs were harvested and isolated from the bone marrow of a donor and provided by CMaT and frozen until needed. To prepare MSCs for seeding, glassware plates were coated with 0.1% gelatin and the MSCs were thawed within a relatively close time frame to maximize the cell viability. Once the MSCs were completely thawed, under a laminar flow hood, the cells were transferred with a 1mL pipette into a sterile 15 mL conical tube. Using a 10 mL pipette, 9 mL of MSC expansion medium prewarmed at 37ºC were added dropwise into the 15 mL conical tube containing the MSCs. The mixture within the 15 mL conical tube was then gently mixed by slowly pipetting up and down twice. The conical tube containing the MSC mixture was then centrifuged at 300 x g for 2-3 minutes to pellet the cells. Decantation of supernatants present within the conical tube was conducted to remove any residual cryo-preservatives. The decanted cells were then resuspended in 10 mL of MSC expansion medium, and the suspended MSCs were placed into a 10-cm

tissue culture plate. The culture containing suspended cell was maintained at 37ºC in a humidified incubator equilibrated with 5% and left there until the next day in which an exchange of the medium with fresh MSC expansion medium pre-warmed at 37ºC was conducted. Once the cell culture was ~90% confluent, they are dissociated with trypsin-EDTA and moved into subcultures for expansion. The medium within the MSC cell subculture was removed and replaced with 5 mL of trypsin-EDTA solution and incubated in a 37ºC incubator for 3-5 minutes. The plate was ensured to have complete cell detachment so that 5 mL of MSC expansion medium could be added to the plate to mix the cell suspension. The dissociated cells were transferred to a 15 mL conical tube and centrifuged at 300 x g for 3-5 minutes to pellet the cells again. The supernatants in the centrifuged cells were discarded and 2 mL of MSC expansion medium containing 8 ng/mL FGF-2 was added to the conical tube and resuspended to the cell. The cells were plated at a density of 10,0000 cells/cm^2 or 40,000 cells/cm^2 into another glass plate with 15 mL of MSC expansion medium containing 8 ng/mL FGF-2. 6 mL of the plated MSC was transferred into a new conical tube to be used for seeding based on the specific cell density.

ME Sensor Gelatin Immersion

To study cell adhesion and growth of MSCs on the surface of magnetoelastic (ME) sensors, six ME sensors were soaked in gelatin prior to cell seeding at differing times. Within a biosafety cabinet, 10 mL of gelatin coating solution 0.1% was pipetted with a 10 mL pipette into a petri dish. Six ME sensors were properly sterilized and four were immersed into the gelatin-containing petri dish. The two ME sensors not soaked in gelatin were labeled as 0 min. – indicative of their absence of gelatin soaking. Of the

ME sensors that were soaked, two were soaked in the 0.1% gelatin for 30 minutes, and the other two were soaked for 60 minutes. The soaked sensors were kept in an incubator (at 37º). Both sensors, after extracting them from the 0.1% gelatin and placing them on top of a carrier stage in a 2-well chamber slide, were properly labeled and marked for the gelatin study. From the results of that study, the eight ME sensors used to study the sensor detection system's ability to track MSC growth were soaked in 0.1% gelatin for 30 minutes, extracted, and prepared using the same procedures as mentioned above.

MSC Seeding

Following standard operating procedures for tissue culture rooms, MSC seeding was conducted in a biosafety cabinet. MSCs were aliquoted into two separate 50 mL conical tubes. One conical tube containing MSCs was diluted to 45,000 cells/ML (for 10,000 cells/cm^2 in the chamber slide) with cell media. The other conical tube containing MSCs was diluted to 180,000 cells/mL (for 40,000 cells/cm^2 in the chamber slides) with cell media as well. 2-well chamber slides were prepared by placing a carrier stage and 0.1% gelatin-coated ME sensor on the carrier stage in the back well. Using a 1 mL pipette, 1 mL of MSCs with a cell. Using a 1mL pipette, 1 mL of MSCs with a cell density of 10,000 cells/cm^2 or 40,000 cells/cm^2 was pipetted on top of each ME sensor in the 2-well chamber slides. After the ME sensors were seeded, they were incubated (at 37ºC) for 30 minutes to allow time for the cells to attach to the ME sensor. After 30 minutes of incubation, their impedance spectra were measured using the sensor detection system and were placed back in the incubator (at 37ºC) for 24 hours.

MSC Fixation and Staining

24 hours after cell seeding and incubation, the MSCs seeded on ME sensors were fixated and stained. Hoechst dye was prepared prior to staining. Hoechst 33342 stock solution was diluted in a 10 mL conical tube with enough PBS – for 0.5 µg of Hoechst 33342 stock solution per 1 mL of PBS – to aliquot 1mL of the diluted Hoechst dye into each 2-well chamber containing the seeded MSCs. The conical tube containing the Hoechst dye is then wrapped in aluminum foil to prevent exhausting the illuminance. Prior to fixation and staining, the impedance spectra of the seeded ME sensors (incubated for 24 hours) were measured again using the sensor detection system. Once the impedance spectra were measured, the 2-well chamber slide containing the MSC seeded ME sensor was sterilized with 70% EtOH and placed within the biosafety cabinet. Each 2-well chamber slide containing MSC seeded ME sensor was aspirated of the remaining MSC media solution present in the well. The well containing the MSC seeded ME senor then had 1 mL of paraformaldehyde (PFA), using a 1 mL pipette, pipetted into it. The PFA remained in the well with the seeded ME sensor for 7 minutes. After 7 minutes, the well was aspirated once again to remove PFA from the well. 1 mL of PBS was then pipetted into the well containing the ME sensor using a 1 mL pipette for the rinsing step. Once rinsed with PBS, the well containing the ME sensor was aspirated again to remove the PBS from the well. 1 mL of the prepared Hoechst Dye was then added to the well containing the ME sensor and put in the incubator (at 37ºC) for 10 minutes. This incubation was to ensure the permeation of the dye into the cells. Once the Hoechst Dye permeated the ME sensor for 10 minutes, it was sterilized and placed back into the biosafety cabinet where it was aspirated from the

well. 1 mL of PBS was then added to the front well (not containing the seeded ME sensor) and the ME sensor from the back well was flipped into the front well – with the carrier stage being discarded. The 2-well chamber slide was then wrapped in aluminum foil to preserve the fluorescence of the Hoechst dye.

Data collection

The impedance spectra of each ME sensor were detected by the sensor detection system. The impedance spectra of each seeded ME sensor were measured 30 minutes after seeding and 24 hours after seeding. All sensors were placed into the AC coil of the sensor detection system. The DC power supply connected to the DC coil provided DC excitation, set at 1.2 amps - based on previous experiments that examined optimal biasing that generated the DC magnetic field that produced the greatest resonance [21]. Data on the sensor's response - magnitude, resonance frequency, and phase - was extracted from the impedance analyzer (Keysight E5061B Network Analyzer). The range of resonance frequency examined was between 160 kHz to 180 kHz based on previous experiments that determined this range to be the expected resonance for ME sensors of the fabricated dimensions [21]. Additionally, 1600 data points were set to be collected for a resolution of 12.5 Hz. A background data point was collected prior to measuring the response of the seeded ME sensors to collect baseline values that would later be used to compare the impedance generated by the ME sensor.

MSC Imaging and Quantification

MSCs seeded on ME sensors were stained with Hoechst dye and imaged using confocal microscopy to analyze the quantity of MSCs attached to the ME sensor. The seeded ME sensor was imaged with Nikon SoRa confocal microscope. The DAPI (4',6-diamidino-2-phenylindole) filter was used to clearly identify and analyze the stained nuclei of attached MSCs. The ME sensor was divided into sections, as seen in figure 3, and images were taken at each section – generating fifteen images that were representative of the cell population attached to the entire sensor. This was repeated for each sensor that was seeded, fixated, and. Once imaged, the cell nuclei on the sensor were annotated and quantified using cell imaging software (ImageJ) to analyze the total number of cells attached to the sensor. This annotation and quantification method was repeated for each image and sensor captured.

	L	M	R
1	L1	M1	R1
2	L2	M2	R2
3	L3	M3	R3
4	L4	M4	R4
5	L5	M5	R5

Figure 3: ME Sensor Imaging Layout

Seeded ME sensors that were fixed and stained had sections of the sensor divided for imaging - highlighted in yellow. This led to 15 different images for each sensor that encapsulated the cell population of the entire ME sensor.

Data processing

Data collected from the impedance analyzer on the sensor response was largely quantitative. Images collected of the cells attached to the sensor were both quantitative and qualitative, in providing the number of cells present on the sensor surface and the morphology of the attached cells. The cell images were quantified using cell imaging software to provide a cell count used for a calibration curve to determine the relationship between sensor response and cell growth.

The calibration curve was processed by plotting the number of cells present on each sensor to the change in magnitude/shift in resonance frequency from the resonance data. Changes in resonance frequency and magnitude of the impedance of the ME sensors were calculated by finding the difference in the sensor's response 30 minutes after seeding compared to 24 hours after seeding.

Results

ME Sensor Gelatin Soaking

To identify whether adhesion preparations were needed to improve cell attachment, ME sensors (n=6) were soaked at different time intervals (0 min., 30 min., and 60 min.) in 0.1% gelatin, seeded with MSCs, fixed, and then stained for cell imaging. It was expected that any gelatin soaking would result in greater cell attachment onto the ME sensor compared to when gelatin soaking was absent. Analysis of the collected data indicated that ME sensors that weren't soaked in gelatin prior to MSC seeding resulted in the fewest number of cells – 317 cells (±45) - attached to the sensor surface (fig. 4a), while ME sensors soaked for 30 minutes averaged 1017 cells (±291) attached to its surface (fig. 4b), and ME sensors soaked in gelatin for 60 minutes had 509 cells (±69) attached to its surface (fig. 4c), respectively. The MSCs seeded across the sensors, soaked in different times, had the same morphology – size and appearance – among themselves. Additionally, gelatin soaking didn't seem to affect the growth and distribution of MSCs across the sensor – remaining relatively heterogeneous in growth but concentrated most heavily at the middle of the sensor – ranging from 38 to 434 cells. Across each sensor, no matter the gelatin soaking time, the sides of the sensors contained the least amount of MSCs attached – ranging from 4 to 43 cells. ME sensor resonance and response weren't collected – or necessary – in determining the effect of 0.1% gelatin preparations.

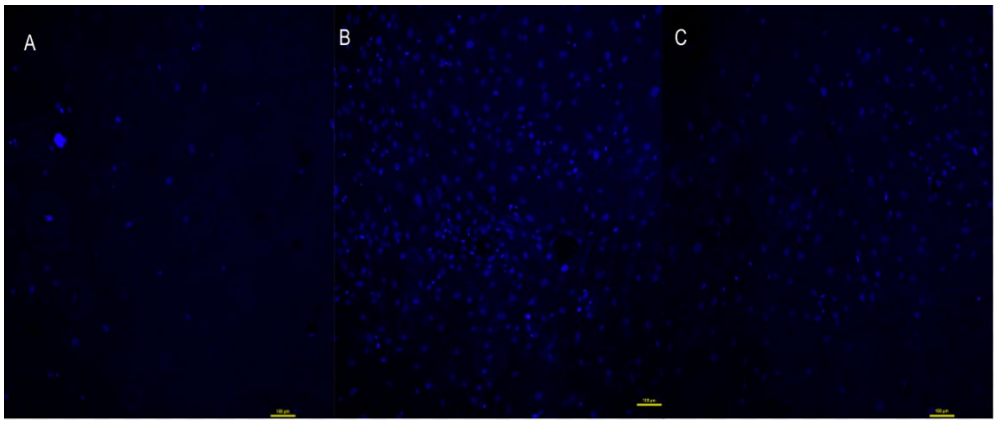

Figure 4: Confocal Images of ME Sensors Soaked in Gelatin at Varying Times

(a) ME sensor soaked in gelatin for 0 minutes. (b) ME sensor soaked in gelatin for 30 minutes. (c) ME sensor soaked in gelatin for 60 minutes.

MSC Impedance

To analyze the ability of the platform to track ME sensor response in respect to MSC growth, 8 sensors (labeled A-H) were resonated 30 minutes after seeding and then again 24 hours after seeding. Sensors A-D were seeded with a density of 10,000 cells/cm2, while sensors E-H were seeded with a density of 40,000 cells/cm2. The ME sensors chosen for this experiment were ensured to have no physical defects, scratch marks, etc. that could affect cell growth and resonance. Additionally, prior to seeding, ME sensors were examined to determine the resonance frequency that they inherently resonate at. ME sensors that resonated at relatively the same resonance frequency were selected for the study for standardization and control. Using the sensor detection system with an excitation applied at 1.2 Amps, it was determined that the selected ME sensors resonated at 170.3 kHz (±1 kHz). Once 30 minutes of incubation after seeding had passed, the ME sensors response resonated at a range of 167.57 kHz – 170.18 kHz. After 24 hours of incubation, after seeding, the ME sensors response resonated at a

range of 169.97 kHz – 167.33 kHz. The shifts in sensor resonance were calculated by finding the difference in its response 30 minutes after seeding compared to 24 hours after seeding. The frequency shifts of the sensors ranged from -12.5 Hz to -237.65 Hz. Sensors A, C, F, and G had the smallest resonance shifts, ranging from -12.5 Hz to -50.13 Hz (fig. 5a). Sensors B, D, E, and H though had larger resonance shifts, ranging from -100.25 Hz to -237.65 Hz (fig. 5b). All the sensors shifted downwards relative to where they initially resonated at, indicative of dampening from mass loading. The magnitude of impedance at the resonance frequency was analyzed from the sensor data collected as well. The magnitude of impedance from the sensors 30 minutes after seeding ranged from - 0.0056 dBm to -0.0030 dBm. Sensors measured 24 hours after seeding had a magnitude ranging from -0.0049 dBm to -0.0025 dBm. The overall change in magnitude from the sensors ranged from 0.00053 dBm to 0.0012 dBm. Sensors A, B, C, D, and G had the smallest change in magnitude, ranging from 0.000382 dBm to 0.000655 dBm (fig. 5a). On the other hand, sensors E, F, and H had the largest change in magnitude, ranging from 0.00112 dBm to 0.00122 dBm (fig. 5b).

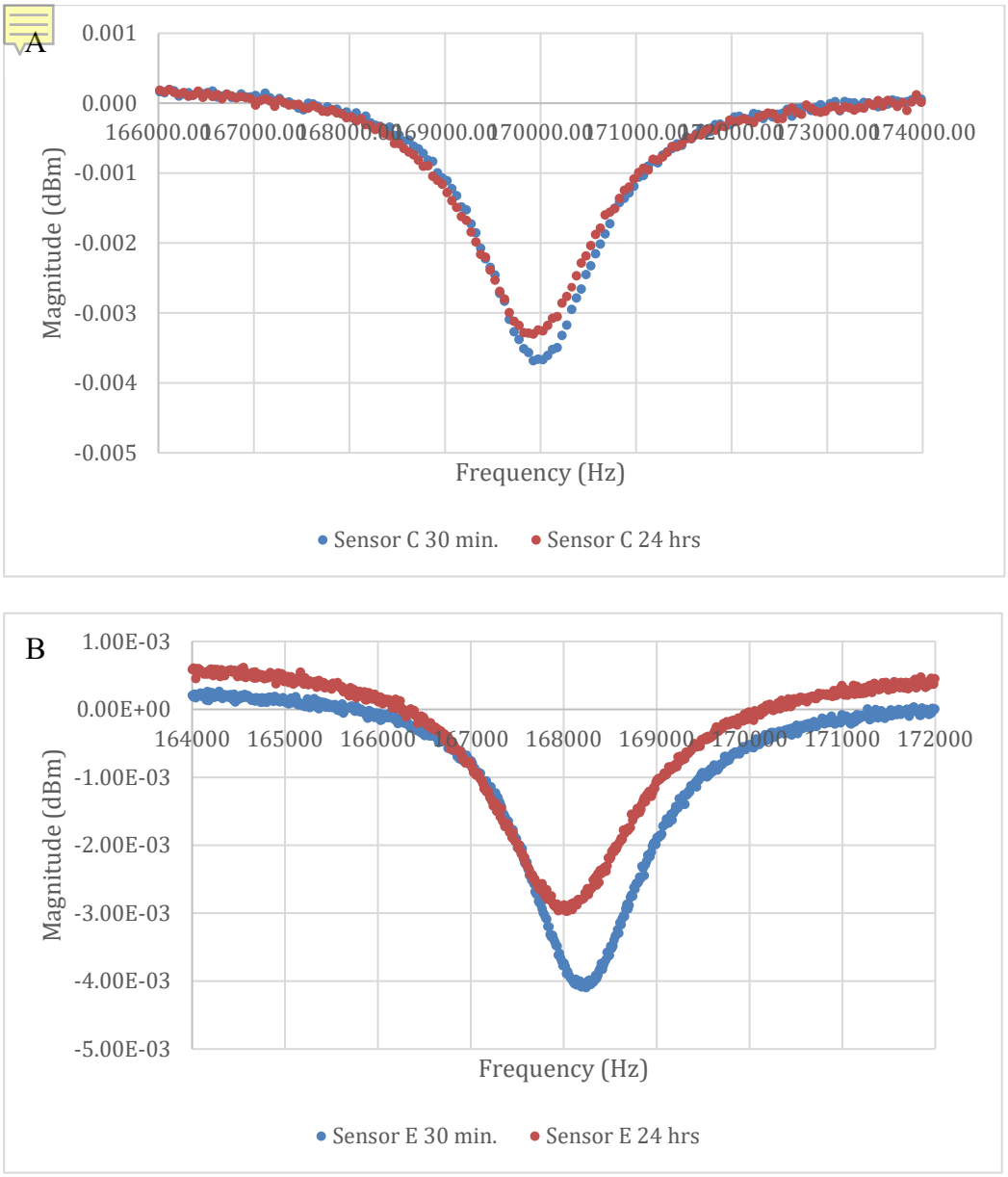

Figure 5: ME Sensors C and E resonance 30 minutes after seeding and 24 hours after seeding

(a) ME sensor C's resonance 30 minutes after seeding and 24 hours after seeding. The sensor experienced a downward shift of -212.63 Hz and a magnitude change of 0.0011 dBm. (b) ME sensor E's resonance 30 minutes after seeding and 24 hours after seeding. The sensor experienced a downward shift of -50.13 Hz and a magnitude change of 0.00038 dBm.

MSC Cell Count

To identify the actual number of cells anchored onto the ME sensors, sensor samples were fixed, stained, and imaged 24 hours after their seeding. Each sensor had 15 images taken of its surface. The stained MSCs present on the surface of the sample sensors was quantified using imaging software and processed to obtain a summation of the number of cells present. To ensure that cells were accurately counted, the cell and nucleus sizes were checked with the scale bar to ensure that they were within typical MSC size of 10 – 30 μm [13]. The sensors had a larger range of MSCs present due to the different seeding densities used (fig. 7). Sensors B and D contained the least number of cells present on its surface, being 744 cells and 793 cells, respectively. Sensor A and C contained 1237 cells and 1268 cells present on its surface. These numbers were predicted as sensors (A-D) were seeded with 10,000 cells/cm^2. Sensor G, on the other hand, despite being seeded with 40,000 cells/cm^2 only had 1436 cells on it. The other ME sensors seeded with 40,000 cells/cm^2 had the greatest number of cells present on the sensor surface – as expected. Sensors E, F, and H had 3809 cells, 3672 cells, and 4052 cells on the sensor surface, respectively.

Additionally, in terms of the morphology of the cells present on the sensor, they were all nearly identical – in terms of their size and shape. The MSCs grown had similar trends of heterogeneous distribution seen previously in the gelatin study with the highest concentration of cells located at the center of the sensor while the edges of the sensors were the least populated areas (fig. 7).

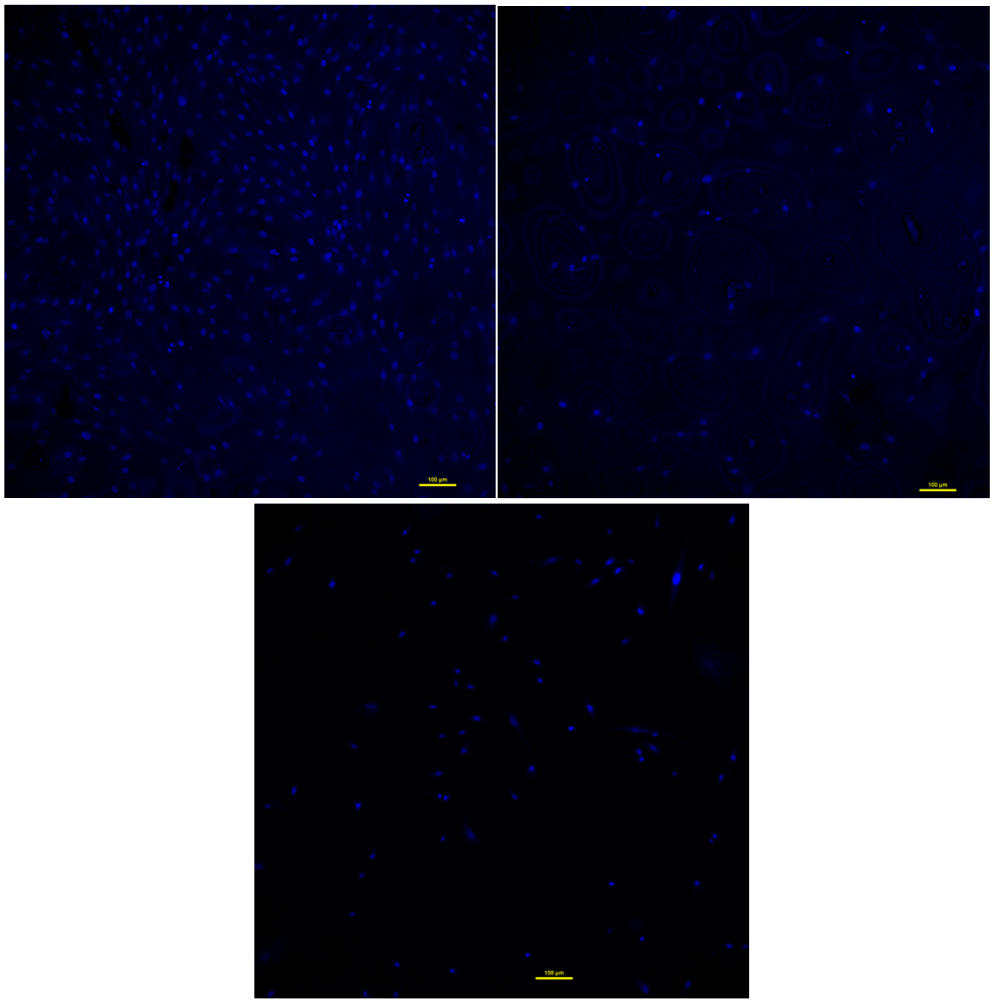

Figure 6: Confocal Imaging of MSCs fluoresced with Hoechst dye
(a) Image of Sensor H at the center of the sensor. Within the image 580 cells were counted. (b) Image of Sensor G at the center of the sensor. Within the image 106 cells were counted. (c) Image of Sensor B at the center of the sensor. Within the image 84 cells were counted.

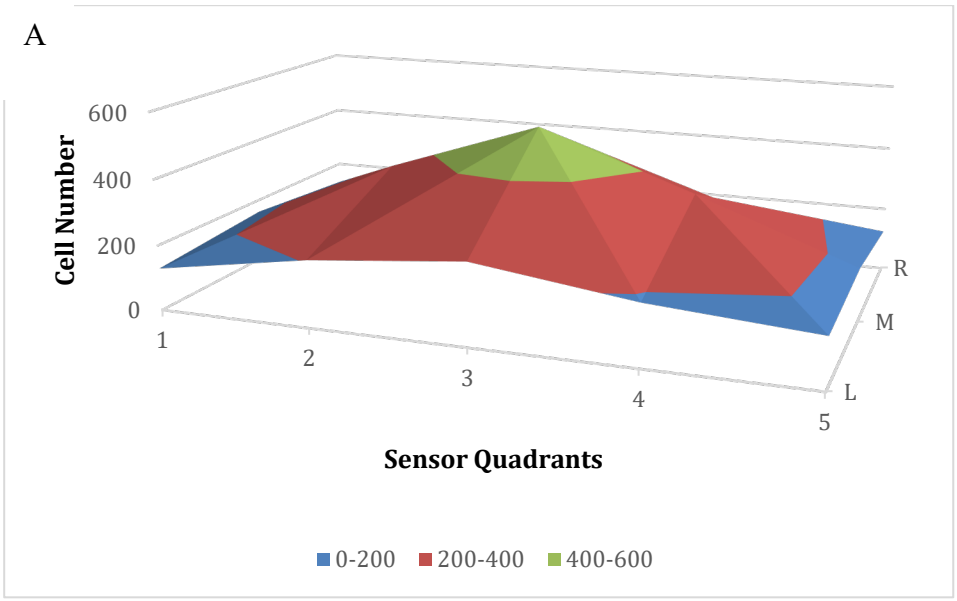

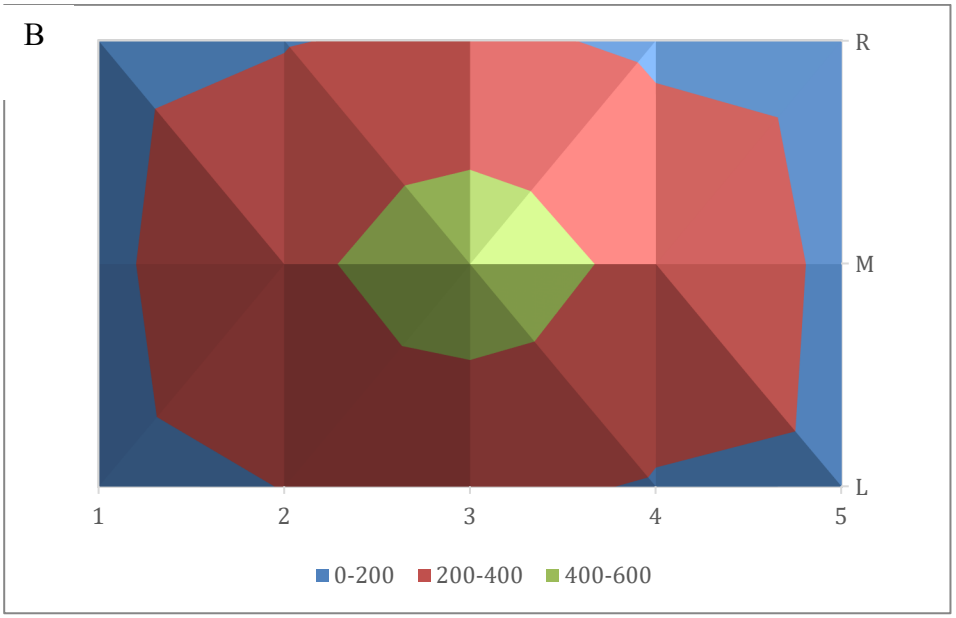

Figure 7: Average Number of MSCs attached to the Sensor Surface

(a)Across the 8 samples, on average, the center of the ME sensor contained the greatest number of MSCs attached while the edges of the sensor contained the least number of MSCs. Sensor quadrants can be referred to figure 3. (b) A top-down view of the sensor confirms that the center of the ME sensor contains the greatest number of MSCs attached.

Discussion and Future Direction

Cell Attachment and Growth

MSCs are anchorage-dependent – needing a surface to support growth – thus, typical culture dishes that support the growth of MSCs contain growth factors and cytokines that resemble a natural niche for stem cells [15]. Magnetoelastic (ME) sensors lack the typical growth serums and cytokines that culture dishes do. In fact, magnetoelastic materials are typically comprised of ferromagnetic metals, which lack organic components that can easily create bonds between their surface and MSCs. This ability to anchor themselves onto the sensor surface is essential for their growth and for monitoring them using the sensor detection system. Additionally, the aim is for the cells to adhere to the sensor surface with enough support to prevent shear stress – or slippage. Unfortunately, including growth factors into the seeding procedures may not guarantee the attachment of the MSCs onto the sensor because it may favor attachment to other surfaces – such as the walls of the chamber slide or the carrier stages. Thus, to address this issue, 0.1% gelatin solution was used to determine whether it would benefit/increase the attachment of MSCs onto the sensor surface. Gelatin is a derivative of collagen and is rich in amino acids, or protein molecules, that can impart structural stability and cell attachment onto cell culture surfaces [5]. By soaking the ME sensors in the 0.1% gelatin solution at varying times, the surface of the ME sensors can be covered in the substrate that can improve MSC attachment after cell seeding. Based on the data points and cell counts collected (at n=6), it was determined that ME sensors soaked in 0.1% gelatin for 30 minutes provided the most optimal setting for cell attachment after seeding (fig. 8)

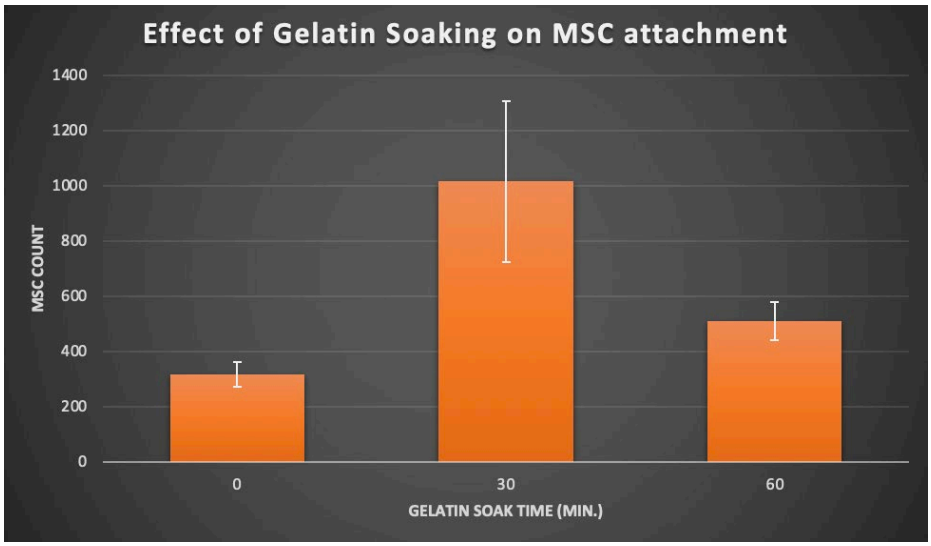

Figure 8: Cell count of ME Sensors Soaked at Varying Times in Gelatin

Quantification of ME sensors soaked in gelatin for 0 minutes, 30 minutes, and 60 minutes. Data collected signify that 30 minute may be optimal time for ME sensors to soak in gelatin to allow for the maximum amount of MSCs to attach onto the sensor surface after cell seeding.

Overall, this examination of ME sensor preparation for cell seeding showed that the inclusion of preparatory 0.1% gelatin soaking improved cell attachment onto the sensor no matter how much time it was soaked. ME sensors not soaked in 0.1% gelatin – denoted as 0 minutes – contained 317 cells (±45 cells), while ME sensors soaked in 0.1% gelatin for 30 minutes contained 1017 cells (±291 cells). While soaking ME sensors in 0.1% gelatin for longer – 60 minutes – shouldn't have harmed or decreased the number of cells attached to the surface, the samples, on average, contained 509 cells (±69 cells) – less than the sensors soaked for 30 minutes. This decrease in cell attachment after a longer soaking time could be due to overcoating of collagen on the ME sensor. Overcoating of collage may eventually lead to the unstable attachment as

the proteins begin to stack on top of each other, causing the seeded MSCs to create attachments onto the collage rather than onto the sensor. The 0.1% collagen acts as scaffolds to aid the MSCs in attaching onto a surface, thus, an excess may block the MSCs from directly attaching onto the sensor. Although the 60-minute soaked ME sensors contained fewer MSCs attached to its surface compared to when it was soaked in 0.1% gelatin for 30 minutes, it was still greater than ME sensors that weren't soaked in gelatin at all. This is indicative that soaking the ME sensors prior to cell seeding benefited its attachment onto the surface of the sensor – crucial in the implementation of this technology as a microcarrier for MSC growth and tracking.

Cell Tracking – Linear Regression Model

The implementation of this sensor tracking platform requires the ability to identify the response of resonated ME sensors and their relationship to the growth of MSCs. The resonated ME sensors all had a response of a downward shift in resonance and decreased magnitude of impedance, indicative of dampening from the sensor. Downward shifts in resonance and dampening of the ME sensors resonance can be due to factors such as changes in temperature, pH, and other biological/chemical parameters that the sensor is exposed to; however, since all other environmental factors – such as temperature – were controlled, this dampening was likely the result of mass loading (or an increase in mass) on the sensor from the growth of MSCs during its 24 hours of incubation of seeding. However, to determine the accuracy, and relationship, between this dampening and the actual number of cells present on the sensor, a calibration curve was processed to show proof of concept that this sensor detection platform can track the growth of MSCs.

To generate this calibration curve, the data points collected from the MSC impedance – resonance frequency, phase shift, the magnitude of impedance – were processed and plotted in relation to the cell count of the respective ME sensor. The phase shift response of the ME sensor wasn't a viable method of tracking cell growth as opposed to the magnitude of impedance and resonance frequency, since its curve was a steep slope which would be a more tedious method of processing this data. The resonance frequency and magnitude of impedance, on the other hand, only required finding the minimum magnitude of impedance and the resonance frequency that it corresponded with – making it more viable for this sensing platform. Shifts in resonance frequency, however, didn't correlate with the number of cells on their corresponding sensor. The generated linear regression line looking at the relationship between the resonance frequency shift of the ME sensor and the sum cell count of its corresponding sensor had an R^2= 0.12. R^2 is the coefficient of determination, which examines how the variation of a dependent variable is predicted by an independent variable. The closer the coefficient is to 1, the more likely the regression prediction fits with the data. Thus, with an R^2= 0.12, resonance frequency shifts aren't a viable predictor of the growth of MSCs on the ME sensor. It can also be concluded that this lack of predictability isn't due to a lack of data points as 1600 data points were collected across a 20 kHz frequency span, collecting data at every 12.5 Hz interval. Thus, using resonance shift at this point isn't a reliable method in tracking MSC growth.

The change in magnitude at the resonance frequency, on the other hand, was a better predictor of MSC growth on the sensor. By finding the linear relationship between cell count and magnitude change, a clearer relationship as the processed

R^2=0.95 (Fig. 9b). This is indicative that analyzing the change in magnitude of the ME sensors response allows the ability to monitor MSCs in this sensor detection system. Furthermore, the change in magnitude can be further concluded to have been caused by the growth of MSCs on the sensor since the environmental factors – such as temperature – was standardized and maintained. Since the collection of ME sensor responses was done so instantaneously (~16 seconds), the response of the ME sensor provided near-instant feedback for real-time tracking of MSC growth. Thus, based on the functionalization of ME sensors set up, this sensing platform can offer an alternative, viable method to monitor the growth of MSCs in 2D cultures. This can offer a rapid response in *in vitro* MSC production to generate optimal – in quality and quantity – products at a faster rate than existing methods.

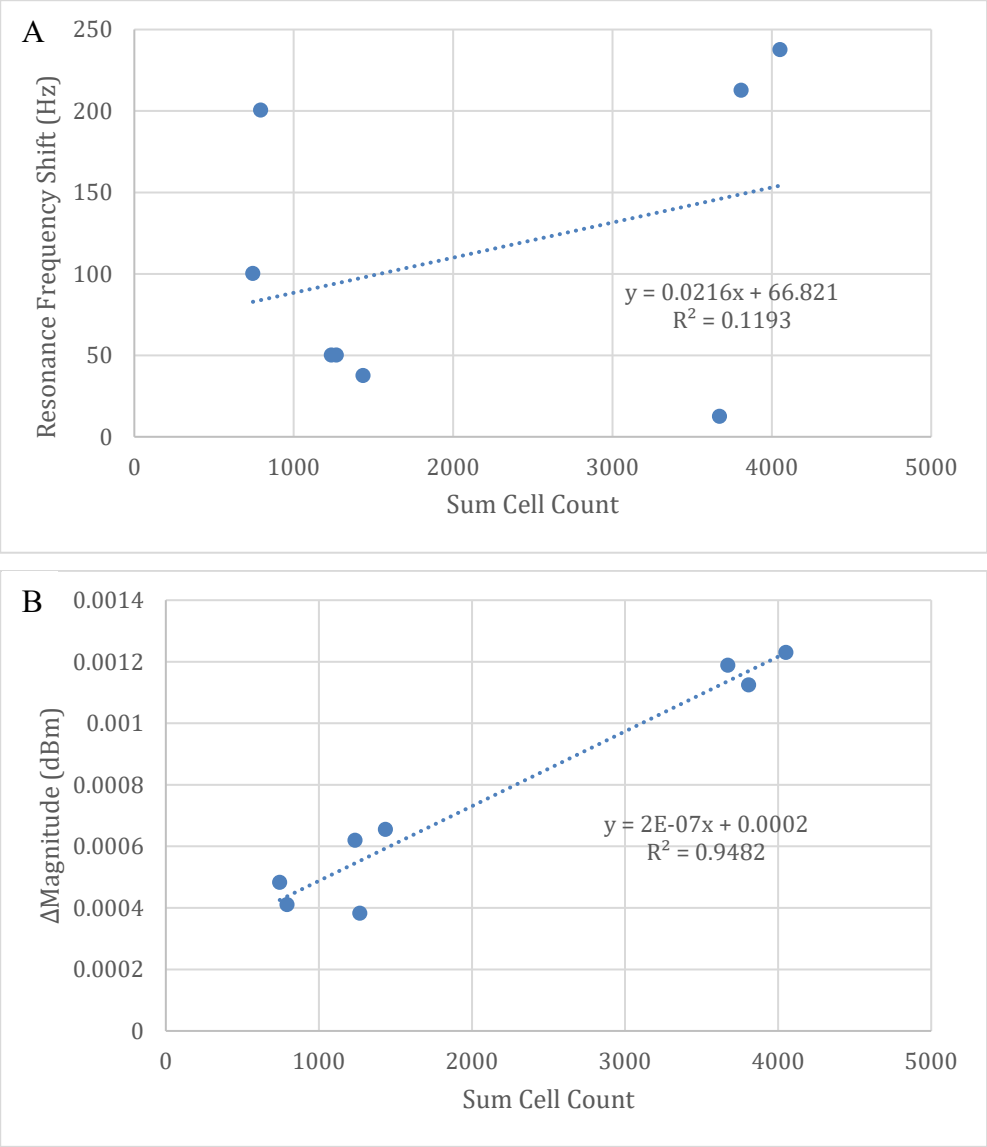

Figure 9: Linear relationships between the number of MSC cells present on the ME sensor samples and data points of measurements

(a) The linear relationship between the sum number of MSCs counted on the ME sensors and the shifts in resonance frequency. R^2 =0.0.12, points are scattered throughout, and no clear trend can be found to identify the relationship between cell number and cell growth. (b) The linear relationship between the sum number of MSCs counted on the ME sensors and the change in magnitude. R^2=0.95, showing a more significant relationship between the change in magnitude of the sensor impedance to the growth of the MSCs.

Future Direction

The results and analysis of this study indicate that ME sensors have the capability to track MSCs in a 2D culture setting and that it can be done so in real-time due to the instantaneous feedback of sensor response. By obtaining data on the magnitude of the impedance of the sensor response as it is resonated in a DC field, any changes in mass loading can be detected by dampening the response. This in turn can monitor the number of cells present on the sensor. This is proof of concept that technology based around ME sensors can be used as a detection platform for the growth of MSCs in culturing techniques. By reducing and minimizing errors and waste, MSCs produced at high volumes can be produced effectively – and in high quality – that increases its availability. This in turn could increase, and improve, research and studies centered around MSCs – potentially allowing for a better understanding of the cells and their abilities to create treatments for injuries and disorders such as bone disease, cartilage deterioration, cardiovascular disease, etc. Additionally, by increasing the availability of MSCs via their production, the cost of the cells for treatment and/or research may be lowered.

Extensions of this study should aim to examine the threshold that this sensing platform can monitor cells accurately and miniaturize/functionalize these ME sensors as microcarriers for the sensing platform. MSCs are typically seeded in cultures at a density of 5,000-6,000 cells/cm2 [16], however, stem cell manufacturing is likely to produce – or aim to contain – cell densities greater than that amount. This study focused on seeding cell density of 10,000 cells/cm^2 and 40,000 cells/cm^2, however, this may even seem minimal compared to the aimed production of some cell manufacturers.

Thus, it is worth extending this study to cell densities greater than 40,000 cell/cm2 and determining the limitations of the ME sensor platform – and the degree of accuracy it has at higher cell densities. Since the intended aim of this technology is to generate a sensing platform that can accurately monitor the growth of MSCs in high volume, it is worth understanding the extent of its accuracy when MSCs are grown in even higher volumes than in this study.

Additionally, the miniaturization of ME sensors and their application to 3D cultures is the next step in developing the use of this technology in cell production. ME sensors can be fabricated to be a variety of sizes – to the scale of micrometers. This flexibility in size can allow for the miniaturization of ME sensors to offer specific areas and optimal settings for cell growth and proliferation during cell production. Microcarriers in 3D cultures that currently exist are on the scale of 100-300 μm. By miniaturizing ME sensors to the micrometer scale, one can further develop their applicability as a microcarrier in MSC production.

Bibliography

1. Centers for Disease Control and Prevention. Underlying Cause of Death, 1999–2018. CDC WONDER Online Database. Atlanta, GA: Centers for Disease Control and Prevention; 2018. Accessed March 12, 2020

2. Chemaly, Elie R., et al. “Tracking Stem Cells in the Cardiovascular System.” Trends in Cardiovascular Medicine, Elsevier, 16 Nov. 2005, www.sciencedirect.com/science/article/pii/S1050173805001805.

3. Chen, Ye, et al. “Mesenchymal Stem Cells: A Promising Candidate in Regenerative Medicine.” The International Journal of Biochemistry & Cell Biology, Pergamon, 16 Jan. 2008, www.sciencedirect.com/science/article/pii/S1357272508000113?casa_token=YdRoc3QSom8AAAAA%3AFz0n3FlUz9tGRQvWo7Bm5b7GJ9jsIuB0Duz7uI0sd3ox8dBiMoq4UC4cj9TouD3p90x8Mh-V.

4. Everhart, J. S., Campbell, A. B., Abouljoud, M. M., Kirven, J. C., & Flanigan, D. C. (2020). Cost-efficacy of Knee Cartilage Defect Treatments in the United States. The American journal of sports medicine, 48(1), 242–251. https://doi.org/10.1177/0363546519834557

5. Gelatin Coating Protocol for Cell Culture (2022, February).MilliporeSigma. https://www.sigmaaldrich.com/US/en/technical-documents/protocol/cell-culture-and-cell-culture-analysis/3d-cell-culture/gelatin-solution-product

6. Grimes, Craig A et al. “Theory, instrumentation and applications of magnetoelastic resonance sensors: a review.” Sensors (Basel, Switzerland) vol. 11,3 (2011): 2809-44. doi:10.3390/s110302809

7. Han, Y., Li, X., Zhang, Y., Han, Y., Chang, F., & Ding, J. (2019). Mesenchymal Stem Cells for Regenerative Medicine. Cells, 8(8), 886. https://doi.org/10.3390/cells8080886

8. Holmes, H. R., DeRouin, A., Wright, S., Riedemann, T. M., Lograsso, T. A., Rajachar, R. M., & Ghee Ong, K. (2014). Biodegradation and biocompatibility of mechanically active magnetoelastic materials. Smart Materials and Structures, 23(9). doi:10.1088/0964-1726/23/9/095036

9. Hmadcha A, Martin-Montalvo A, Gauthier BR, Soria B and Capilla-Gonzalez V (2020) Therapeutic Potential of Mesenchymal Stem Cells for Cancer Therapy. Front. Bioeng. Biotechnol. 8:43. doi: 10.3389/fbioe.2020.00043

10. Institute of Medicine (US) Committee on a National Surveillance System for Cardiovascular and Select Chronic Diseases. A Nationwide Framework for Surveillance of Cardiovascular and Chronic Lung Diseases. Washington (DC): National Academies Press (US); 2011. 2, Cardiovascular Disease. Available from: https://www.ncbi.nlm.nih.gov/books/NBK83160/

11. Justice, C et al. “Online- and offline- monitoring of stem cell expansion on microcarrier.” Cytotechnology vol. 63,4 (2011): 325-35. doi:10.1007/s10616-011-9359-4

12. Kircher, Moritz F, Gambhir, Sanjiv S, and Grimm, Jan. "Noninvasive Cell-tracking Methods." Nature Reviews. 8.11 (2011): 677-88. Web.

13. Lipowsky, H. H., Bowers, D. T., Banik, B. L., & Brown, J. L. (2018). Mesenchymal Stem Cell Deformability and Implications for Microvascular Sequestration. Annals of biomedical engineering, 46(4), 640–654. https://doi.org/10.1007/s10439-018-1985-y

14. Mason, Chris et al. “Cell therapy industry: billion dollar global business with unlimited potential.” Regenerative medicine vol. 6,3 (2011): 265-72. doi:10.2217/rme.11.28

15. Merten O. W. (2015). Advances in cell culture: anchorage dependence. Philosophical transactions of the Royal Society of London. Series B, Biological sciences, 370(1661), 20140040. https://doi.org/10.1098/rstb.2014.0040

16. Mesenchymal Stem Cell Culture Protocols (2022, February). MilliporeSigma. https://www.sigmaaldrich.com/US/en/technical-documents/protocol/cell-culture-and-cell-culture-analysis/stem-cell-culture/mesenchymal-stem-cell-culture-protocols

17. Meyers KM, Ong KG. Magnetoelastic Materials for Monitoring and Controlling Cells and Tissues. Sustainability. 2021; 13(24):13655. https://doi.org/10.3390/su132413655

18. Mizukami, A., & Swiech, K. (2018). Mesenchymal Stromal Cells: From Discovery to Manufacturing and Commercialization. Stem cells international, 2018, 4083921. https://doi.org/10.1155/2018/4083921

19. Odeleye, A., Castillo-Avila, S., Boon, M., Martin, H., & Coopman, K. (2017). Development of an optical system for the non-invasive tracking of stem cell growth on microcarriers. Biotechnology and bioengineering, 114(9), 2032–2042. https://doi.org/10.1002/bit.26328

20. Qiyue Wang, Xibo Ma, Hongwei Liao, Zeyu Liang, Fangyuan Li, Jie Tian, and Daishun Ling, “Artificially Engineered Cubic Iron Oxide Nanoparticle as a High-Performance Magnetic Particle Imaging Tracer for Stem Cell Tracking.” ACS Nano, pubs.acs.org/doi/10.1021/acsnano.9b08660.

21. Shekhar, S.; Karipott, S.S.; Guldberg, R.E.; Ong, K.G. Magnetoelastic sensors for real-time tracking of cell growth. Biotechnol. Bioeng. 2021, 118, 2380–2385.

22. Simon, Carl G., et al. “Strategies for Achieving Measurement Assurance for Cell Therapy Products.” Stem Cells Translational Medicine (AlphaMed Press), John Wiley & Sons, Ltd, 21 Apr. 2016, stemcellsjournals.onlinelibrary.wiley.com/doi/full/10.5966/sctm.2015-0269.

23. Thavorn, K., van Katwyk, S., Krahn, M., Mei, S., Stewart, D. J., Fergusson, D., Coyle, D., & McIntyre, L. (2020). Value of mesenchymal stem cell therapy for patients with septic shock: an early health economic evaluation. International journal of technology assessment in health care, 36(5), 525–532. https://doi.org/10.1017/S0266462320000781

24. Ullah, Imran et al. “Human mesenchymal stem cells - current trends and future prospective.” Bioscience reports vol. 35,2 e00191. 28 Apr. 2015, doi:10.1042/BSR20150025